The Application of TM Imagery and GIS Data in the Assessment of Arid Lands Water and Land Resources in West Texas

Paul Neville, Robert I. Coward, Richard P. Watson, Michael Inglis, and Stan Morain

Abstract

The objective of this research was to develop an image-based geographic information system (GIS) that could help evaluate ground water quality and land development potential in the Salt Basin of Trans-Pecos Texas. The stimulus for this effort was to evaluate whether the groundwater geochemistry and soil surface chemistry could be determined using commercial, off-the-shelf, geo-spatial technology. If so, these tools could be used to determine the commercial value of land and water for agricultural, industrial, and municipal purposes. The results are promising. Landsat Thematic Mapper imagery, used in conjunction with the geospatial databases, allowed areas to be identified that showed a potential for good-quality groundwater with arable land suitable for multiple uses. Image maps were produced to characterize the surface and subsurface attributes, and were used by the commercial partner to evaluate land development potential.

Introduction

The objective of this research, as proposed by Cassidy Energy, was to use off-the-shelf remote sensing and geographic information system (GIS) technologies to analyze the surface and hydrologic resources in the Salt Basin, Texas for improved land-use planning. The Trans-Pecos Texas is notable for its arid climate and limited surface water. For decades, people in this area have depended for economic support on the cyclical markets of cattle, irrigated agriculture, oil, and gas. Many of the large, enclosed basins within this region are underlain by groundwater reserves, but these waters are of highly varying quality. These resources have remained largely unexploited until recently due to poor infrastructure and the sparse population of the region. However, less than 90 miles west of the Basin are the cities of Las Cruces, El Paso, and Ciudad Juarez. The lifeline for this tri-city region is the Rio Grande (Hibbs *et al.*, 1997). As the combined population of these cities swells, the ability of the Rio Grande to supply water demands will decline. It is not surprising that developers are turning their eyes to the Salt Basin for its groundwater potential. El Paso, which relies heavily on groundwater, is considering alternatives such as using agricultural water for municipal uses. Throughout the Trans-Pecos region, groundwater is becoming an increasingly valuable commodity requiring active management planning.

Procedures and information derived from this project were intended to assist Cassidy Energy to help rural Trans-Pecos communities in their planning process to analyze the surface and hydrologic resources of the area. The study focused on the Salt Basin as representative of arid basins throughout the Trans-Pecos region. The goal was to produce an image-based GIS application for evaluating land parcels and their associated groundwater and surface resources for potential economic development.

Three specific research questions were developed based on the assumption that groundwater in the Salt Basin is likely to reflect the chemical properties of the surface materials. These questions derive from the geological conditions that define the drainage pattern and geochemical environment of the Salt Basin. The technical questions addressed by this study included

- can the chemical properties of surface soils be detected using low-cost, easily accessible multispectral image data;
- can surface spectral responses be used as an indicator of groundwater chemistry; and
- can discontinuous point data from wells be combined with spatially explicit spectral data in a GIS to assist economic decisions related to water quality and land use?

The Affiliated Research Center (ARC) project partner for this research was Cassidy Energy, Inc. based in Midland, Texas. Cassidy Energy is a natural resources exploration and development company with an on-going interest in oil, gas, and water resources analyses in the Trans-Pecos region of New Mexico and West Texas. Recent corporate initiatives include the evaluation of the application of geospatial and spectral technologies to the analysis of these resources.

The Study Area

The Salt Basin is a large, internally drained basin trending from northwest to southeast and measuring approximately 100 kilometers by 30 kilometers (Figure 1). The basin is defined by mountain ranges on all sides except to the northwest were it meets the gently sloping Diablo Plateau. The greatest relief of the basin occurs along the northeast margin where it abuts the Guadalupe Mountains that rise to an elevation of 2667 meters. The flat basin floor averages 1100 meters in elevation.

The winters in the project area are mild with low temperatures averaging −12° C (Boyd and Kreitler, 1981). The summers are hot and dry with temperatures rising to 46°C.

Annual precipitation ranges from 21 cm in the Basin to over 50 cm in the Guadalupe Mountains. Evaporation regularly

---

P. Neville, R.P. Watson, M. Inglis, and S. Morain are with the Earth Data Analysis Center, University of New Mexico, Bandelier West Room 111, Albuquerque, NM 87131-6031 (rwatson@spock.unm.edu).

Robert I. Coward is with Cassidy Energy, Inc., P.O. Box 50162, Midland TX, 79710-0162.

Photogrammetric Engineering & Remote Sensing
Vol. 66, No. 11, November 2000, pp. 1373–1379.

0099-1112/00/6611–1373$3.00/0

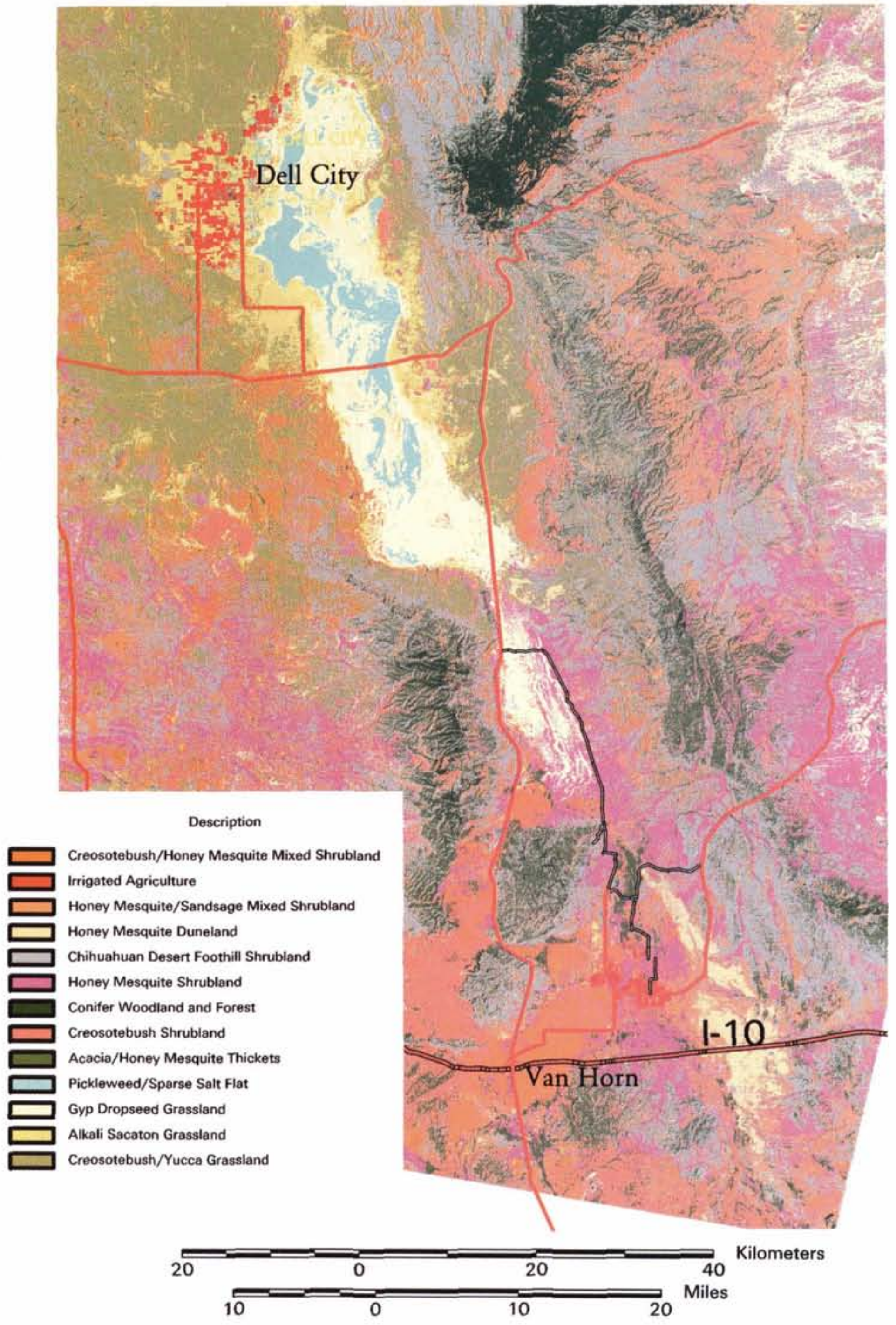

Plate 1. Land-cover map of the study area.

exceeds available moisture, with almost all of the groundwater recharge coming from the surrounding mountains. Because the Basin drains internally, rainfall that is not lost to evapotranspiration is captured as groundwater, and over time accumulates at depth. This recharge filters through Permian and Cretaceous marine carbonate and evaporite complexes, creating groundwater conditions that can range from freshwater to water rich in dissolved sulfate and chloride minerals. Wicking and evaporative mechanisms on the surface have resulted in large areas of gypsum sands surrounding smaller saltpans.

Vegetation mirrors moisture availability. Most of the area is sparsely covered by xeric plants typical of the Chihuahuan Desert, mainly creosote bush (*Larrea tridentata*) and low-growing acacia (*Acacia spp.*). The more xeric areas are dominated by gypsophile plants such as gyp dropseed (*Sporobolus nealleyi*) and halophile plants such as pickleweed (*Allenrolfea*

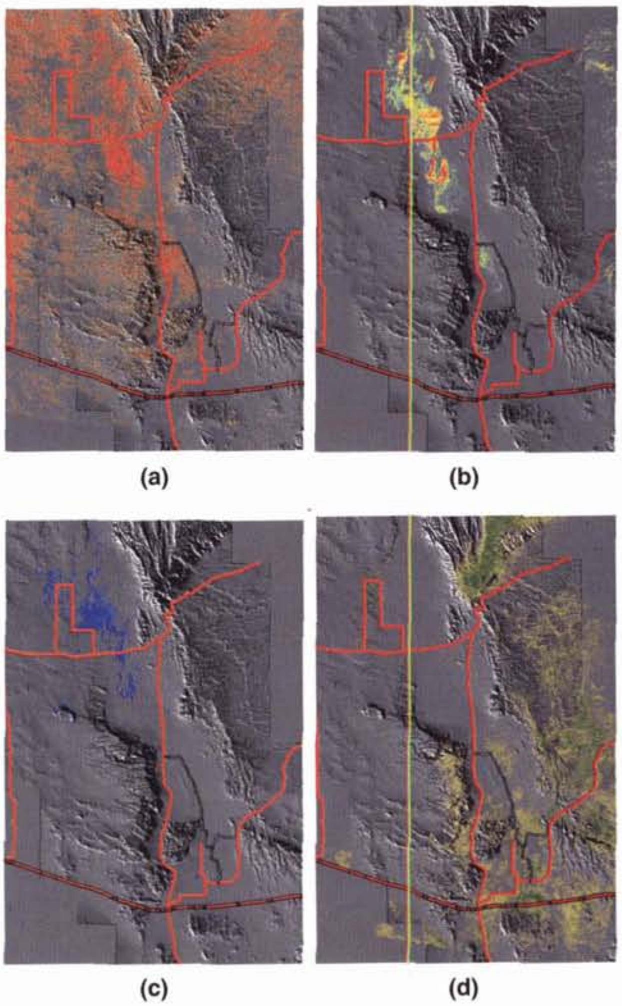
(a) (b)

(c) (d)

Plate 2. The EM image with values exceeding 300 in red (a), the GI image (surface gypsum image) color coded from blue to red (b), the surface salt image showing locations of surface salt deposits in blue (c), and the greenness vegetation index with highest values in dark green (d).

occidentalis). Only in the higher mountains are the natural conditions sufficiently mesic to support woodland and forest communities dominated by one-seed juniper (*Juniperus monosperma*) and piñon pine (*Pinus edulis*). Other naturally mesic areas within the Basin include arroyo riparian communities supporting honey mesquite (*Prosopis glandulosa*) and acacia thickets. Irrigated agricultural fields and residential lawns constitute artificially mesic sites.

The project focused on the two small towns that occur within the confines of the basin, Dell City in the north and Van Horn in the south. Dell City (population—569) has a long history of irrigated agriculture from wells. The groundwater in this district is saline to very saline, to the extent that municipal water has to be treated through an electrodialysis desalination plant. The groundwater chemistry of Van Horn (population—2,240) is less saline than that of Dell City. Unlike Dell City, Van Horn has a more diverse economic base with less dependence on irrigated agriculture.

Methods

Database Development

Image processing, GIS, and GPS (Global Positioning System) technologies were used to produce data sets for analysis and interpretation. A Landsat 5 Thematic Mapper (TM) image, acquired on 13 May 1995, was used as the base image. ERDAS Imagine™ v.8.3 software was used to process this image. The image was calibrated using the gain and offset values from the header data. The image was then rectified to a Universal Transverse Mercator Projection, Zone 13, using the 1927 North American Datum, Clarke 1866 Spheroid. The image was resampled using the nearest-neighbor method to preserve the spectral-radiometric integrity of the data.

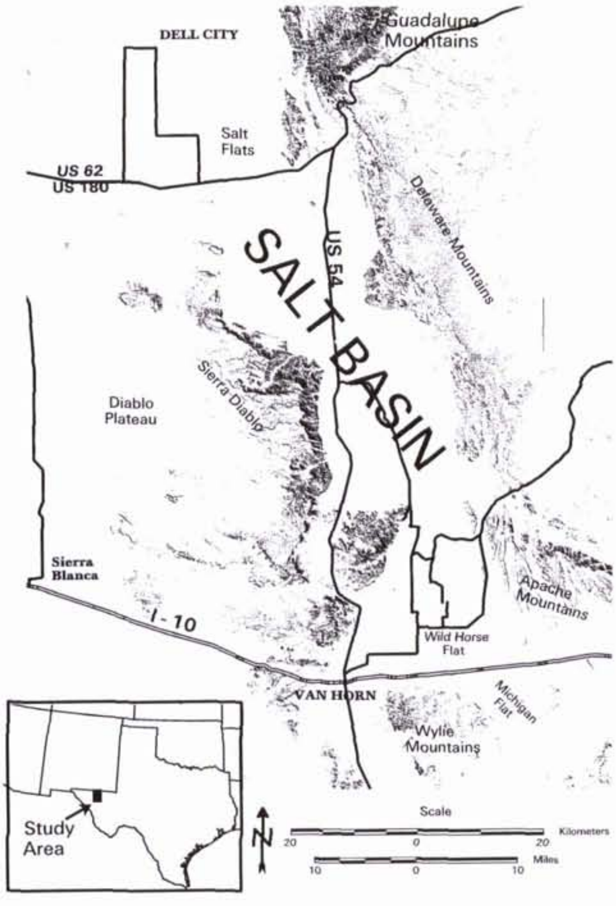

Figure 1. Study area.

Road and hydrology networks (1:24,000-scale Digital Line Graph data) were downloaded from the U.S. Geological Survey Internet site. These themes were appended and edited in ERDAS Imagine™, ESRI's ARC/INFO™ v. 7.2.1, and ArcView™ v.3.2 software. Geology was digitized from the Van Horn-El Paso 1:250,000-scale geologic map sheet in the Geologic Atlas of Texas (Bureau of Economic Geology, 1983).

Well data from the Texas Water Development Board (TWDB)(URL:**http://www.twdb.state.tx.us/Newwell/well_info.html**) were downloaded and converted into Arc/Info coverages and ArcView shapefiles. The TWDB site provided data on over 1,400 county wells for Hudspeth and Culberson counties. The majority of these wells are concentrated in the Dell City and Van Horn areas, respectively.

Field Data Collection

Field data collection involved the assessment of vegetative ground cover, soil sample collection, and measurements of electromagnetic inductance. Vegetation was assessed using image classification and field verification at selected sites in the project area. Soils were sampled for subsequent laboratory analysis from 25 locations, including those evaluated for electromagnetic inductance. Data on soil conductivity were collected at 17 sites using an electromagnetic inductance device. This device has a 4-m-long PVC housing that covers transmitting and receiving coils located at opposite ends of the device (Hendrickx *et al.*, 1992). The transmitting coil induces small currents in conductive soil that are then sensed by the receiving coil. The receiver intercepts parts of the electromagnetic field that are reflected from the terrain. These readings are measured in millisiemens/meter (mS/m). The highest conductivity readings (greater than 1,000 mS/m) occur in the Basin salt flats, with lower readings (less than 30 mS/m) occurring throughout the remainder of the study area.

Image-Derived Data

To address the technical questions defining this research, several sources of image-derived data were developed. Measures of vegetative ground cover, electromagnetic inductance, and surface salt deposits were derived using the TM imagery. These data provided the basis for the analysis of groundwater quality and potential land use.

Vegetation Classification

A land-cover classification was developed to provide a base map of land-cover types and their extent. The analysis of land cover was also examined as a possible indicator of surface and groundwater quality. The land-cover classification map was created using a maximum-likelihood classification from 53 field-based training locations. These locations were described in the field and located using GPS. The resultant classification was recoded to 13 generalized land-cover classes (Plate 1) to characterize the landscape into more meaningful categories.

EM Inductance Index

Electromagnetic (EM) inductance was used to test whether higher soil conductivity can be used as a proxy for increased dissolved solids in groundwater. Site locations for EM inductance measurements were chosen using the TM image and by selecting relatively homogeneous vegetative or soil-cover regions. These site locations and the EM values were converted into a GIS point coverage using GPS coordinates. The TM spectral radiance values at these locations were then matched to their corresponding EM values through a multiple regression model to create an equation to predict the EM values throughout the image. The resulting equation had an R^2 value of 0.85 and was highly significant (F equals 0.0037). The regression equation is shown in Equation 1: i.e.,

$$\mathrm{EI} = 1498.13 + (124.3 * \mathrm{TM1}) - (322.769 * \mathrm{TM2}) + (78.72 * \mathrm{TM3}) + (10.97 * \mathrm{TM5}). \tag{1}$$

where EI is the derived EM image. The visible bands (TM1, TM2, and TM3) were the most significant bands. Positive loadings in TM1, TM3, and TM5 indicate an enhancement of bright soil response.

Surface Gypsum Index

An image illustrating the surface extent of gypsum was considered to be important due to its implications towards both quantifying arable surface potential and its possible effect on groundwater quality. This image was generated using a Feature-Oriented Principal Components Analysis of selected TM bands similar to a technique used by Loughlin (1991). Landsat TM bands 1, 4, 5, and 7 were chosen because they emphasize known gypsum absorption features and reflectance peaks (Bowker *et al.*, 1985). Component 3 of the resultant eigenmatrix had the expected pattern, with positive loadings for TM1 and TM5 and negative loadings for TM7 and TM4. The first three component loadings match the spectral responses for gypsum, with positive loadings on TM1 and TM5 corresponding to reflectance peaks for gypsum, while the negative loading for TM7 corresponds to absorption of mid-infrared energy by the hydroxyl molecule. The negative loading on TM4 separated this component from a similar response expected for well-watered, healthy vegetation. These component loadings were used in Equation 2 to generate the gypsum-derived image (GI): i.e.,

$$\mathrm{GI} = (0.147 * \mathrm{TM1}) - (0.163 * \mathrm{TM4}) + (0.536 * \mathrm{TM5}) - (0.815 * \mathrm{TM7}). \tag{2}$$

Greenness Index

Because vegetation mirrors water availability, it was determined that an assessment of greenness might contribute to the delineation of areas having sufficient surface water or near-surface groundwater to sustain vegetative growth. A greenness index was derived from the TM image by using the tasseled cap transformation (Crist and Cicone, 1984). This transformation is created by applying pre-set coefficients that reduce dimensionality of the image data to bands representing brightness, greenness, wetness, and haze. The tasseled cap greenness vegetation index (GVI) coefficients for Landsat 5 data are shown in Equation 3; i.e.,

$$\mathrm{GVI} = (-0.2728 * \mathrm{TM1}) - (0.2174 * \mathrm{TM2}) - (0.5508 * \mathrm{TM3}) + (0.7221 * \mathrm{TM4}) + (0.0733 * \mathrm{TM5}) - (0.1648 * \mathrm{TM7}). \tag{3}$$

Results

Image Analysis

The analysis of the image-derived data yielded results useful in the assessment of the link between surface geology, vegetation cover, and groundwater quality and potential land use. These data provided information on the distribution and extent of surface salts and vegetation throughout the project area. A comparison of field conditions to the image classification found that the classified image accurately portrayed the actual land cover within the project area. The image-defined classes provide accurate indications of the surface properties and offer a basis for the assessment of potential land use of the area. Each of the land-cover classes was characterized according to its dominant vegetation type and landscape characteristics based on field verification. The land-cover classes illustrated in Plate 1 represent the field verified and aggregated image classes.

The acacia/honey mesquite thickets (olive drab) represent arroyo riparian communities where groundwater is close to the surface. The gyp dropseed grassland (pale yellow) community shows where the soils are gypsic. The sparse pickleweed/salt flat (blue-gray) community shows the extent of the salt flats whereas the alkali sacaton grassland (khaki) community shows where soils may still be saline. These grasslands may have areas of good forage, but, given the extreme physical and chemical environments in which they are located, they can be sensitive to overuse and subject to deterioration. The honey mesquite duneland (beige) and honey mesquite/sandsage mixed shrubland communities indicate where soils may not be stable enough for most potential land uses. The other shrublands have a variety of soil and forage conditions, lending themselves to a variety of uses including grazing or even irrigated agriculture where water is available. The creosotebush/yucca (*Yucca spp.*) grasslands (khaki) dominated by blue grama (*Bouteloua gracilis*), black grama (*Bouteloua eriopoda*), and bush muhly (*Muhlenbergia porteri*) can have good forage value, but tend to occur on thin, rocky soils. The Chihuahuan Desert Foothill shrubland (gray) communities are sparsely vegetated with ocotillo (*Fouquieria splendens*), agave (*Agave spp.*), and prickly pear cactus (*Opuntia spp.*) dominated by rock outcrops. This classification provided a basis for a potential land-use map. Suitability for use for farming and grazing, both individually and in combination, were assessed for each of the defined land-cover classes.

The derived EM image (Plate 2a) enhanced the saltpans and gypsum flats found in the Basin as well as areas to the northeast of the study area that were found to be Permian-age Castille evaporites (Bureau of Economic Geology, 1983). The sparsely vegetated Diablo Plateau, to the west of the study area, also shows high values in this image. These values are attributed to the widespread presence of limestone outcrops in the plateau.

The gypsum image corresponds well with the approximate location of surface gypsum deposits in the Salt Basin (Plate 2b). The highest brightness values in this image occur in the north and central portions of the Salt Basin where the gypsum sands are found. In addition, high brightness values are present to the northeast and east of the basin where the Castille Formation evaporites outcrop (Bureau of Economic Geology, 1983). Soil samples confirmed this gypsum response pattern. Based on these results, the highest values in this image accurately model the spatial extent of gypsum on the surface. This image also identifies several areas of human-related anomalies, although they are below the threshold used to identify substantial gypsum deposits. These anomalies were traced to the use, 20 years ago, of anhydrous ammonia in agricultural fields.

By modifying the equation used to calculate the gypsum image, it is also possible to model the saltpans that occur in the middle of the gypsum playa. This equation is identical to that used to create the gypsum image with the exception of the use of a negative loading on TM1. The differentiation of the saltpans may be the result of a general similarity of the spectral responses in the IR wavelengths, but with a reduced response in the visible blue spectrum due to an increase in soil moisture. Shown in blue on Plate 2c, saltpans are concentrated to the east and southeast of Dell City. This image corresponds well to the known saltpans in the Basin. Both the gypsum image and the saltpan images readily identify the targeted surface salt deposits.

The tasseled cap greenness vegetation index resulted in an image that enhanced areas of healthy, well-watered vegetation (Plate 2d). It was expected that the greenness index would enhance areas where vegetation has access to surface water or near-surface groundwater, especially as the image was acquired during the hot, dry season for this area. The results were mixed in this regard. Areas with irrigated agriculture, the more mesic conifer woodlands and forest, and the arroyo riparian did show the brightest responses. Most of the higher greenness response is found in the southern part of the Basin. This area, according to the classification and confirmed on the ground, is dominated by shrubland vegetation types, especially honey mesquite, which maintain green leaves in the late spring in contrast to the warm season grasslands which are still senescent and therefore not directly related to surface moisture conditions at the time of image acquisition.

GIS Analysis

The assessment of potential land use, and groundwater quality and distribution was undertaken in a GIS using the image-derived data sources and the water quality data provided by the Texas Water Development Board. The water quality attributes of interest were Total Dissolved Solids (TDS), sulfate, chloride, and Sodium Absorption Ratio (SAR). The TDS values were characterized by standard water usability thresholds, with fresh water classified as less than 1,000 mg/l, slightly saline ranging between 1,000 to 3,000 mg/l, and above 3,000 mg/l classified as saline (Figure 2). Similarly, sulfate and chloride concentrations were classified with values above 300 mg/l classified as "high." The SAR is a measure of the sodium exchange capacity, in which values higher than 6 indicate more saline water. Most of these variables mirror each other in relative concentrations, with the Van Horn area having mostly fresh to slightly saline water, whereas the Dell City water was mostly saline. The wells with the highest salinity occur in the north and central parts of the Basin.

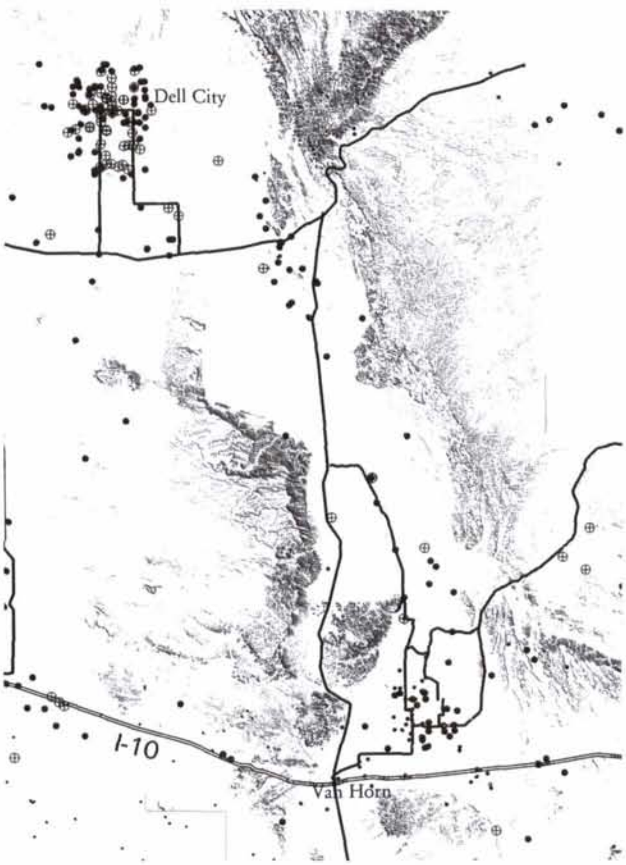

Figure 2. TDS values with freshwater shown as small dots, moderately saline water as larger dots, and very saline water as dots with cross-hairs.

The GIS analysis involved the comparison of the water quality values to the image-derived data in order to determine if the EM, GI, and/or the Salt Image were useful to predict groundwater quality. The assessment of the EM image yielded mixed results. Wells near the Basin center and on the Diablo Plateau to the west had some of the highest concentrations for each of the water quality variables, i.e., were most saline. These wells correspond well with high values in the EM image. However, not all areas were as suggestive of a clear-cut relationship. For example, wells near areas of active agriculture are much more problematic. In these areas, all water quality values are elevated, apparently as a result of the active pumping of irrigation water rather than as a function of surface land cover/composition.

The ability of the gypsum and salt images to identify surface salts suggested that perhaps they would also indirectly model groundwater sulfate and chloride concentration levels, respectively. Results, however, suggest that image data accurately portray the surface cover/composition but do not reliably provide a model of groundwater quality. While, as initially expected, it might be reasonable to assume a connection between surface characteristics and geochemistry, and groundwater quality, evidence from the Salt Basin does not support such a conclusion.

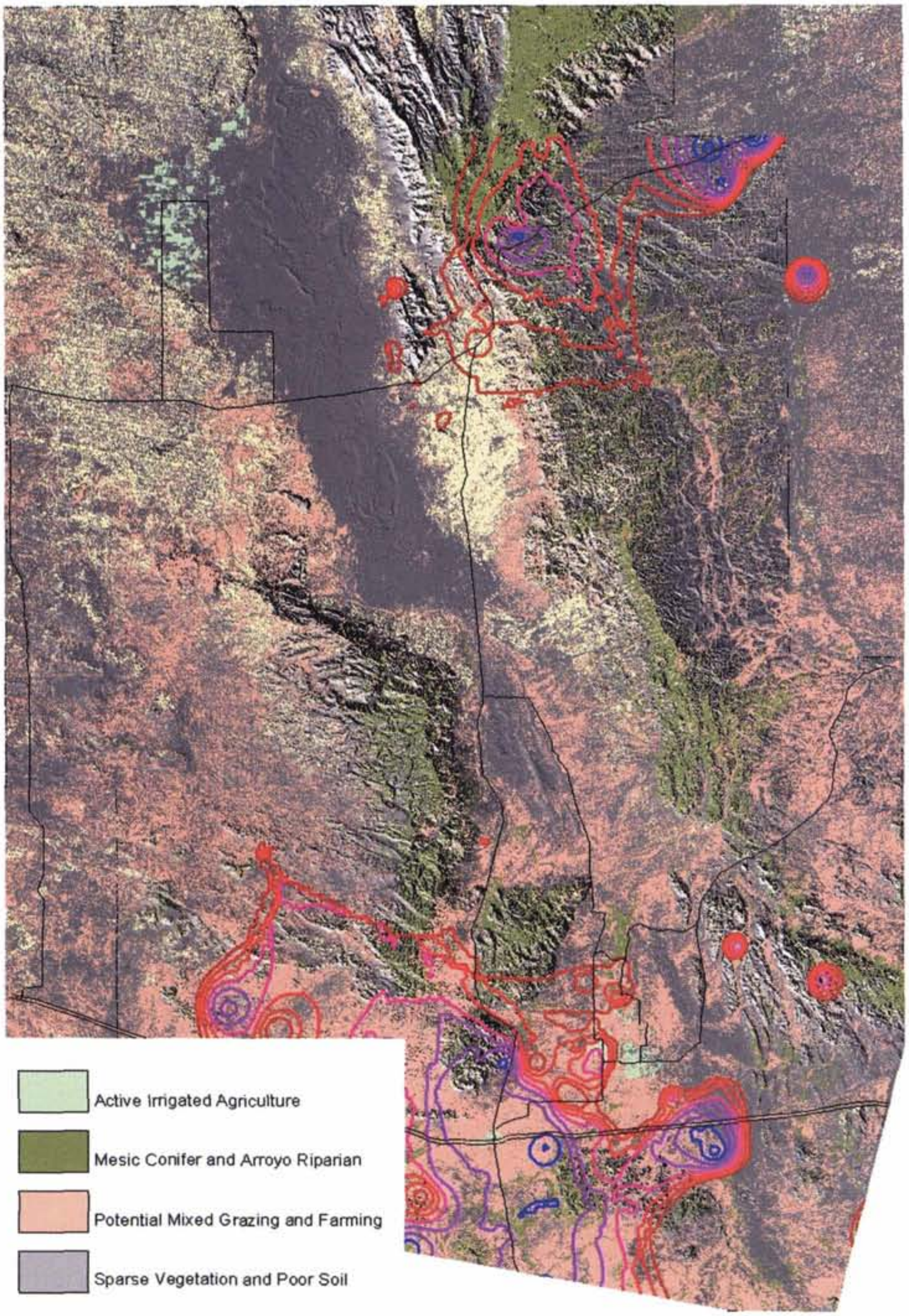

Plate 3. *Potential best land-use image with active agriculture as pale green, potential grazing use in yellow, potential mixed grazing and farming use in tan, mesic conifer and arroyo riparian communities in green, and areas with sparse vegetation cover or poor soil conditions in gray. Contours based on TDS level with blue to red representing increasing TDS values until they reach the moderately saline threshold in red.*

Nonetheless, the EM, gypsum, and salt images provided useful maps of surface properties important for land-use decisions. These images were used in a model with the potential land-use image to mask out areas of sparsely vegetated or poor soil conditions. The resulting image shows that the largest area of arable land is in the southern part of the Basin. Contours developed from each of the water quality attributes for the most part show the same general trend as shown with the TDS variables (Plate 3). The combination of these varied data demonstrates that the southern part of the basin holds the most promise for both good water quality and arable land. Cassidy Energy is presently using this information to concentrate their development and planning efforts in this part of the basin.

Conclusions

The results of the project are encouraging, if not entirely expected. Landsat imagery and GIS databases were used to characterize and assess groundwater geochemistry and soil characteristics of the Salt Basin. In some areas, the soil chemistry matches the groundwater chemistry, but in others, there appears to be a disjunction between the soil chemistry and groundwater quality. These results indicate that, even in areas of deep alluvium such as the Salt Basin, it is not possible to consistently model groundwater quality from multispectral satellite data. The analysis of the image and vector data sets, however, point to the southern third of the Salt Basin as the area with the best combination of water and land-cover characteristics most suitable for development. In this area, there is the potential for a source of fresh groundwater with nearby arable land that can be used for a variety of agricultural purposes. Further research needs to be undertaken to understand better the local and regional geography and the extent of groundwater reserves. Future development of the project database will include the incorporation of land parcel data to allow users to quickly assess the economic potential of individual locations.

Metrics

The procedures and database developed by this project provided a valuable new tool to Cassidy Energy, Inc. As a direct result of this project, Cassidy has now expanded their efforts as consultants to several small water conservation districts in West Texas. Cassidy Energy has further extended their endeavors to include research on the long-term environmental impacts of land- and water-use changes in the Trans-Pecos. An understanding of how geospatial technologies, such as remote sensing and GIS, can be applied to these issues has led Cassidy Energy to further expand their efforts to aid local communities in their economic development and planning. Through Cassidy Energy, Inc. the application of modern spectral and spatial technologies to the assessment of potential land and water use is bringing a new and far-reaching perspective to the rural communities of West Texas.

Acknowledgments

The authors thank the NASA Earth Science Enterprise Commercial Remote Sensing Program at Stennis Space Center for sponsoring the Affiliated Research Center Program at the University of New Mexico, Earth Data Analysis Center. They also thank Dr. Jan Hendrickx for the use of the EM-31, Aaron Brotman and Julie Woolslayer for their assistance in the field, and Michael Lacyk for GIS support. In addition, they would like to thank Teri Neville and Thomas K. Budge for their assistance in reviewing this manuscript.

References

Bowker, D.E., R.E. Davis, D.L. Myrick, K. Stacy, and W.T. Jones, 1985. *Spectral Reflectances of Natural Targets for Use in Remote Sensing Studies*, NASA Reference Publication 1139, National Aeronautics and Space Administration, Scientific and Technical Information Branch, Washington, D.C., [for sale by the National Technical Information Service, Springfield, Virginia], 181 p.

Boyd, F.M., and C.W. Kreitler, 1981. Hydrogeology of a Gypsum Playa, Northern Salt Basin, Texas, *Bureau of Economic Geology Report of Investigation No. 158*, University of Texas Press, Austin, Texas, pp. 1–36.

Bureau of Economic Geology, 1983. Van Horn-El Paso Sheet, 1:250,000 scale, *Geologic Atlas of Texas*, University of Texas Press, Austin, Texas (1 sheet).

Christ, E.P., and R.C. Cicone, 1984. Application of the Tasseled Cap Concept to Simulated Thematic Mapper Data, *Photogrammetric Engineering & Remote Sensing*, 50(3):343–352.

Hendrickx, J.M.H., B. Baerends, Z.I. Raza, M. Sadig, and M.A. Chaudhry, 1992. Soil-Salinity Assessment by Electomagnetic Induction of Irrigated Lands, *Soil Science Society of America Journal*, 56(6):1933–1941.

Loughlin, W.P., 1991. Principal Component Analysis for Alteration Mapping, *Photogrammetric Engineering & Remote Sensing*, 57(9):1163–1169.

Hibbs, R.J., R.N. Boghici, M.E. Hayes, J.B. Ashworth, 1997. *Transboundary Aquifers of the El Paso/Ciudad Juarez/Las Cruces Region*, prepared by the Texas Water Development Board, the New Mexico Water Resources Research Institute, the Comisión Nacional del Agua, Ciudad Juárez (Mexico), the Junta Municipal de Agua y Saneamiento de Ciudad Juárez, and the International Boundary & Water Commission (United States and Mexico) for the U.S. Environmental Protection Agency, Region VI, The Texas Water Development Board, Austin, Texas, 148 p.